Evaluation of Factors Affecting Tibial Bone Strain after Unicompartmental Knee Replacement

Elise C. Pegg,[1] Jonathan Walter,[2] Stephen J. Mellon,[1] Hemant G. Pandit,[1] David W. Murray,[1] Darryl D. D'Lima,[3] Benjamin J. Fregly,[2] Harinderjit S. Gill[1]

[1]Nuffield Department of Orthopaedics, Rheumatology and Musculoskeletal Sciences, Nuffield Orthopaedic Centre, University of Oxford, Oxford, UK, [2]Department of Mechanical and Aerospace Engineering, University of Florida, Gainesville, Florida, [3]Shiley Center for Orthopaedic Research and Education, Scripps Clinic, La Jolla, California

Received 18 May 2012; accepted 5 November 2012
Published online 28 November 2012 in Wiley Online Library (wileyonlinelibrary.com). DOI 10.1002/jor.22283

ABSTRACT: Persistent pain is an important cause of patient dissatisfaction after unicompartmental knee replacement (UKR) and has been correlated with localized tibial strain. However, the factors that influence these strains are not well understood. To address this issue, we created finite element models to examine the effect on tibial strain of: (1) muscle forces (estimated using instrumented knee data) acting on attachment sites on the proximal tibia, (2) UKR implantation, (3) loading position, and (4) changes in gait pattern. Muscle forces acting on the tibia had no significant influence on strains within the periprosthetic region, but UKR implantation increased strain by 20%. Strain also significantly increased if the region of load application was moved >3 mm medially. The strain within the periprosthetic region was found to be dependent on gait pattern and was influenced by both medial and lateral loads, with the medial load having a greater effect (regression coefficients: medial = 0.74, lateral = 0.30). These findings suggest that tibial strain is increased after UKR and may be a cause of pain. It may be possible to reduce pain through modification of surgical factors or through altered gait patterns. © 2012 Orthopaedic Research Society. Published by Wiley Periodicals, Inc. J Orthop Res 31:821–828, 2013

Keywords: finite element; pain; simulation; unicompartmental; knee

While both total knee replacement (TKR) and unicompartmental knee replacement (UKR) are generally successful treatment options, unexplained pain remains an issue and is one of the most common causes of dissatisfaction and revision.[1] Persistent pain after knee replacement is also more common than after hip replacement.[2] The multifactorial nature of pain makes identifying the etiology challenging. Some authors have theorized that excessive strain within bone may stimulate nociceptor activity and cause pain.[3,4] Simpson et al.[4] correlated a typically painful region on the tibia, identified in patients after UKR, with increased von Mises strain (VMS) using finite element (FE) analysis. However, the study only modeled articular contact forces, and loading from the muscles at their tibial attachment sites was not included.

Accurate estimation of muscle contact forces is difficult due to indeterminacy in the musculoskeletal system. This indeterminacy arises from having more unknown muscle forces than available equations from rigid body dynamics.[5] The most common methods for estimating muscle forces omit inclusion of articular contact models and assume that muscles alone contribute to the net knee flexion-extension moment from inverse dynamics.[6,7] Consequently, articular contact loads are not factored into the muscle force estimation process, which may result in inaccurate muscle force estimates. Through the use of an instrumented knee prosthesis that can directly measure the force distribution between the condyles, Fregly et al. developed a 12 degree-of-freedom (dof) knee model that can resolve articular contact and muscle loads simultaneously.[8]

We used FE simulations to examine the role that muscle forces, contact forces, and surgical factors play in determining tibial strain after UKR. Four hypotheses were tested: that the addition of muscle forces to the simulation does not significantly affect tibial strain; that implantation of a UKR increases tibial strain; that malpositioning of the femoral component does not affect tibial strain; and that tibial strain can be changed by gait modification.

METHODS

Estimation of Muscle and Joint Contact Forces

A single subject (male, BMI: 22.5, 83 years, neutral alignment) implanted with a force-measuring tibial prosthesis[9] performed overground walking trials at a self-selected speed.[10,11] These trials included the subject's normal gait pattern and a medial–lateral trunk sway gait pattern intended to modulate medial contact force.[12] The two patterns were selected for the simulations that investigated the effect of gait on tibial strain. Contact forces applied to the medial and lateral sides of the tibial tray were collected simultaneously with ground reaction, surface marker motion, and electromyographic (EMG) data. Knee kinematics estimated from the marker motion data were adjusted such that medial and lateral contact forces calculated by an elastic foundation contact (EFC) model of the subject's implant components reproduced the experimentally measured contact forces.

Muscle force estimates for 13 muscles crossing the knee were generated using a subject-specific 12 dof knee model and static optimization.[8] Tibiofemoral and patellofemoral contact forces were modeled using an EFC model.[13] The knee

Additional supporting information may be found in the online version of this article.

Grant sponsor: NIH; Grant number: R01EB009351.

Elise C. Pegg present address is Nuffield Department of Orthopaedics, Rhematology and Musculoskeletal Sciences, Nuffield Orthopaedic Centre, University of Oxford, Oxford, OX3 7LD.
Correspondence to: Elise C. Pegg (T: +44-1865-227663; F: +44-1865-227671; E-mail: elise.pegg@ndorms.ox.ac.uk)

model was identical to the one published by Lin et al. [8] except that it was built in the OpenSim[14] environment utilizing its inverse dynamics and moment arm analyses. Muscle attachments and wrapping surfaces were taken from a generic cadaver-based model[15] and transformed onto the subject-specific geometry. Muscle force was modeled as peak isometric force times activation, with activation modeled as simulated EMG shifted by a muscle-common time delay and raised to a muscle-specific power between 0.5 and 1.[6]

The static optimization minimized errors between simulated and measured muscle EMG patterns (available for 9 of the 13 muscles modeled), and constrained the estimated muscle forces to balance the net superior-inferior force, varus-valgus moment, and flexion-extension moment at the knee. These net loads were calculated from inverse dynamics with contributions from contact forces eliminated.[16] Outputs from the knee model were contact force magnitudes, directions, centers of pressure, and areas in the medial and lateral compartments, along with muscle force magnitudes, directions, and application points on the tibia. Included muscles were the three vastii muscles, the rectus femoris, semimembranosus, semitendinosus, sartorius, gracilis, and tensor fasciae latae.

Preparation of the Geometry

Using our previously validated methodology,[17] computed tomography (CT) scans of a 60-year-old subject (male, BMI: 25.9) were segmented using Mimics software (version 14.1, Materialise, Leuven, Belgium) to create the tibial geometry. An iterative closest point (ICP) algorithm[18] was used to register this tibia model with the one used to calculate muscle forces (MATLAB, Version 7.10, MathWorks Inc., Natick, MA), thereby allowing mapping of the muscle attachment sites. The tibia model was prepared for implantation of an Oxford UKR mobile bearing knee (Biomet UK Ltd., Bridgend, UK) in accordance with standard operative techniques[19] using Boolean operations (SolidWorks CAD software, Version 2011–2012, Waltham, MA). A sagittal cut to a depth of 4 mm below the medial plateau of the bone was made in line with the mechanical axis of the tibia and was positioned at the medial edge of the tibial spine. At the same depth anteriorly, a transverse cut was made with a 7° posterior slope. The tibia was also truncated 100 mm below the medial plateau to reduce the overall model size. Use of a shortened tibial model has been validated previously.[4]

The cuts resulted in two regions: the cut region and the main tibial region. In models that examined the tibia prior to UKR (hereafter referred to as the Native model), these two regions were bonded together using a tie constraint. For the simulations of the UKR, the cut portion was removed from the simulation, and the main tibial region modeled with the components inserted (hereafter referred to as the Implanted model). For the Implanted model, a 1 mm cement gap was simulated between the tray and the tibia, and the tray was implanted in the center of the cut plateau. The bearing was positioned 1 mm from the wall of the tray and in the center of the plateau along the AP direction. The femoral component was aligned with the axis of the central peg normal to the surface of the tibial tray (Fig. 1).

Finite Element Mesh Definition

The two regions were meshed separately; thus the mesh of the main part of the tibia was identical for all models. A mesh sensitivity study was performed on the Native model without muscle forces. Mesh sizes from 3.8 to 2.2 mm were assessed. Mesh convergence was defined as the point at which the VMS was within 95% of the strain of the next two smaller mesh sizes. This criterion was met by a mesh size of 2.4 mm, giving 70,402 elements for the tibia (Fig. 2). All the implanted Oxford UKR components were meshed using a mesh size of 2.0 mm, with a total of 14,924 elements for the tibial component. Ten node tetrahedral elements were used throughout.

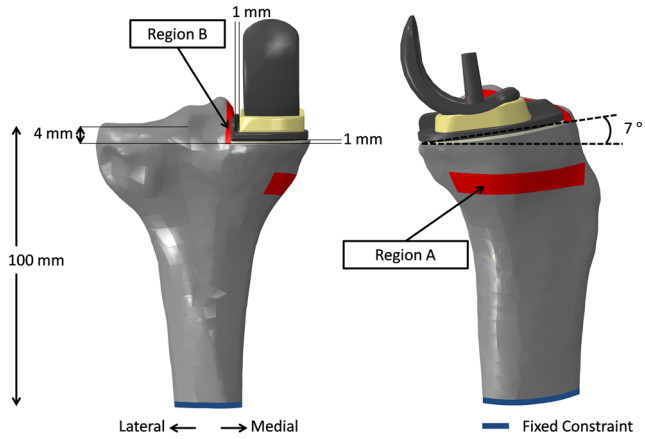

Figure 1. Illustration of the placement of cuts for the implantation and the position of the components. The periprosthetic analysis regions are highlighted in red. The AP and ML views are shown.

Boundary Conditions for the Finite Element Model

Static implicit FE models were created using ABAQUS (version 6.11, Simulia, Providence, RI). A spatially varying value of elastic modulus (E) was used, with the value for bone regions being calculated from the Hounsfield units in the CT scan. A Poisson's ratio of 0.3 was assigned for all elements; the material property assignment was performed with Mimics. The equations used for the relationship were those defined and validated previously[17]; 400 material assignments

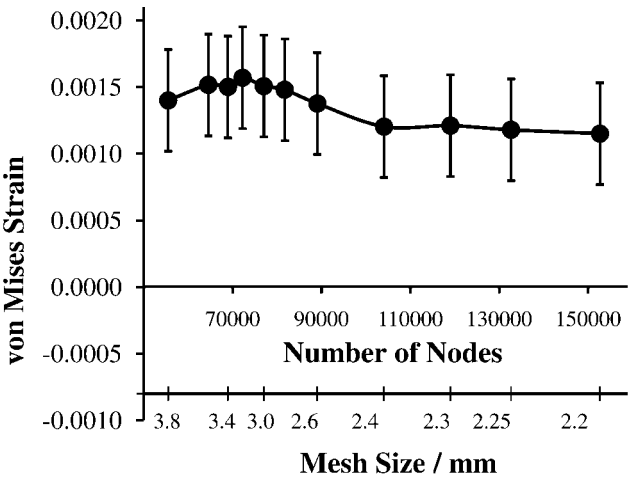

Figure 2. Dependence of the mean von Mises strain in Region A on the number of nodes in the model. The von Mises strain met the mesh convergence criteria at a mesh size of 2.4 mm (104,053 nodes). Error bars represent the standard deviation in the data.

Table 1. Material Properties Assigned to Implanted Oxford UKR Components

Material	Part(s)	Young's Modulus (MPa)	Poisson's Ratio
PMMA	Cement	1,940[20]	0.40[24]
UHMWPE	Bearing	940[2]	0.46[2]
CoCrMo alloy	Femur	195,000[20]	0.30[8]
CoCrMo alloy	Tibial Tray	195,000	0.30

were used (E range, 0.01–17 GPa, consistent with previous work[17]). All implant components were modeled as linear elastic isotropic materials (Table 1). In the Implanted model, tie constraints were used for the tray-cement and cement-bone interfaces.

For the Native model, joint contact forces were applied directly to the tibial plateau. Joint contact forces measured experimentally varied in magnitude, direction, position, and contact area throughout the two gait cycles examined. A custom python script (Python version 2.7, Python Software Fdn) was written to identify elements within the calculated contact area (modeled as circular[20]) around the center of pressure for the medial and lateral sides of the tibia; the load was uniformly distributed across this area. Muscle loads were also applied in the same manner using the areas specified by musculoskeletal model. Loads of appropriate magnitude and direction were applied to the tibia for the contact and muscle forces at each normalized location in the gait cycle (5% gait cycle intervals); these locations were modeled as a series of steps.

For the Implanted model, joint contact forces were applied to the plateau using an analytically mapped field[21] with the same pressure distribution that would be caused by a femoral component loading a polyethylene bearing. The pressure distribution was calculated from a simulation including the bearing and the femur (Equation 1), where P_n is the force applied to node n, P is the total medial load, and x_n is the radial distance of the node from the bearing center:

$$P_n = P(-0.0014x_n + 0.747) \quad (1)$$

During gait, the center of the analytically mapped field was positioned at the center of pressure given by the EFC model. If the center of pressure would cause the bearing position to be beyond the tray wall, lateral movement was constrained.

Post-Processing

The VMS in two periprosthetic regions was found: a region defined on the exterior medial proximal cortex (Region A, 219 elements) examined in previous studies,[4] and a region 2 mm lateral from the wall of the tray where radiolucency is often observed (Region B, 123 elements, Fig. 1). As VMS is not a standard ABAQUS output, it was necessary to modify the input file using a custom Python script. The VMS was calculated by dividing the von Mises stress for each element by its elastic modulus. The use of identical meshes for the main portion of the tibia enabled difference plots of the change in VMS (ΔVMS) to be created with a custom Python script.

Assessment of Difference

To evaluate the differences in VMS among the various FE models, a probabilistic statistical approach was used.[22] The error in load magnitudes calculated by the musculoskeletal knee model were previously assessed[8]; the root-mean-squared (RMS) errors were 10 N for contact forces and 15 N for muscle forces. Given these errors, custom Python scripts were created that introduced equivalent artificial variability into the contact and muscle loads applied to the FE models, where the variability was assumed to be normally distributed. The Implanted model under normal gait cycle loading was then run 40 times, each time with a different randomly created error for each load at each stage of the cycle. The variability in the results from these 40 tests was then used for statistical analyses.

The mean VMS within the specified regions (A or B) was calculated for each of the 40 models and the 40 results treated as one dataset. Statistical analyses were then performed, using either a Kruskal–Wallis test to compare multiple factors at once or a Mann–Whitney *U*-test to compare two datasets. Spearman's rho was used to assess correlation, and a multiple linear regression model was used to examine the significance of factors on the VMS (PASW Statistics, version 18.0.0, SPSS, Inc., Chicago, IL).

Model Verification

To ensure that the contact loading method chosen did not affect the FE results, we assessed the influence of three loading methods: applying the contact load through the femoral component and bearing (Verification Model A), applying it directly onto the tray using an analytically mapped field (Verification Model B), and applying it directly onto the tray using the same method as for loading the Native model (Verification Model C). No significant difference was found in the results from the three methods (S-Fig. 2). Thus, the analytically mapped field was used to compare with previous studies.[4]

The use of a tie constraint to model the bonding at the interfaces is a simplification, as these surfaces are predominantly bonded by a macro-geometric fit. A more complex model was created, which used a friction coefficient of 0.3 between the cement and the tray[23] and a rough interaction between the cement and the bone (Verification Model D). No significant strain difference was found between the model where the cement was tied and when a contact condition was used. Finally, a full length tibial model was created to assess whether analysis of just the proximal portion changed the result (Verification Model E); no significant differences were found between the shortened and the full length tibial models.

Summary of Simulations

The simulations were organized into groups designed to test our four hypotheses: (1) the effect of muscle loads on tibial strain, (2) the change in strain after UKR, (3) the effect of bearing and femur (analytical loading) position on strains, and (4) the change in strain caused by varying gait pattern (Table 2). In simulations (2) and (3), the data at 16% of the normal gait cycle were used, as this was when loading of the medial compartment was maximal. Muscle forces acting on the tibia were included in simulation 2–4, and to the relevant models for simulation 1. The effect of load position changes was examined using increments of 1 mm in the ML direction and 2 mm in the AP direction. The load could be moved only

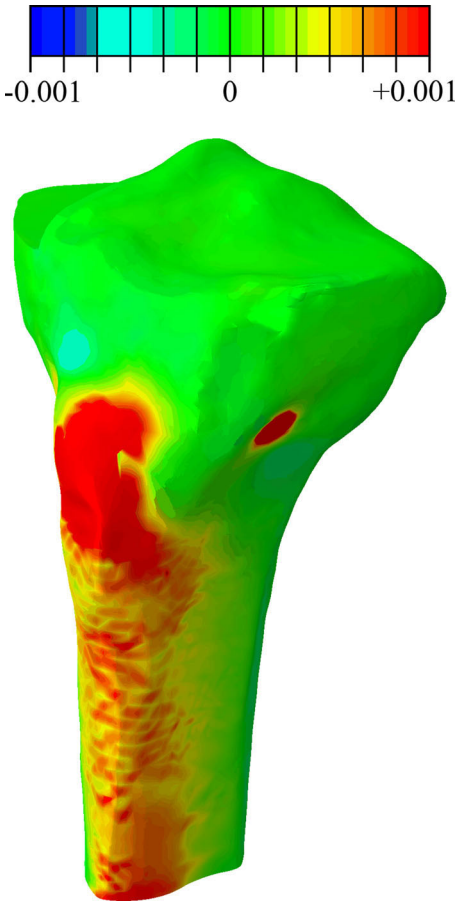

Figure 3. The distribution of ΔVMS is illustrated for loading conditions at 20% of the gait cycle.

1 mm in the lateral direction due to the bearing being constrained by the wall of the tibial tray.

RESULTS

During the majority of the normal gait cycle, the addition of muscle forces caused a localized increase in strain at the attachment sites on the tibia (Fig. 3). This effect was particularly noticeable for the vastii and rectus femoris (via the patellar ligament) and the tensor fascia latae. However, the addition of muscles did not cause any significant changes in strain within the periprosthetic region (Fig. 4) at any stage of the gait cycle (Table 3, $p < 0.05$).

After UKR strain increased in two regions: the corner between the sagittal and transverse cuts, and in Region A (Fig. 5). The mean VMS in Region A significantly increased ($p = 0.0012$) by 24.6% (849.7 με native tibia, 1058.6 με implanted tibia). The strain within Region B decreased by 16.2% but this change was not significant ($p = 0.138$).

Movement of the loading position away from the center, beyond 12 mm anteriorly or 10 mm posteriorly, caused a significant increase in the mean VMS in Region A ($p < 0.035$). The strains increased to a 20% higher level in the posterior direction (14 mm posterior, 1716.6 με) compared with the anterior direction (14 mm anterior, 1425.8 με; Fig. 6a, S-Fig. 6a—animation). Movement of the load position >3 mm medially from the center significantly increased the mean VMS ($p < 0.008$). The strain increased by 900 με for every 1 mm of movement in the medial direction (Fig. 6b, S-Fig. 6b—animation).

A linear correlation was found between the joint contact load (both medial and lateral) and the VMS in the periprosthetic regions for both gait patterns (Fig. 7). The correlation coefficient was higher for the medial load (0.961) than with the lateral load (0.792), but both were significant ($p < 0.01$). Multiple linear regression showed that both medial and lateral load affected the VMS, but that the effect from medial load was greater (standardized regression coefficients: medial load = 0.739, lateral load = 0.298).

Significant differences in the VMS in Region A were found at certain stages of the gait cycle when comparing the two gait patterns (Fig. 8). Particularly significant differences were found in the VMS during push-off (40–50% gait cycle, $p < 0.00004$); this was the stage when the VMS was maximal for both gait patterns. At this stage the peak VMS during lateral trunk sway gait (1011.5 με) was 6% lower compared with the normal gait pattern (1075.3 με). Significant differences were also found at the end of terminal-stance (90–100% gait cycle, $p < 0.03$); at this stage the peak VMS during lateral trunk sway gait (497.7 με) was 50% lower compared with the normal gait pattern (248.3 με).

DISCUSSION

This study investigated four factors that could influence tibial bone strain, and therefore pain, following

Table 2. Summary of the Simulations Performed; (1) the Effect of Muscle Loads on Tibial Strains, (2) the Change in Tibial Strains After UKR, (3) the Impact of Loading Position on Tibial Strains, and (4) the Difference in Tibial Strain With Varying Gait

Test	Models	Gait Pattern	Part of Cycle	Muscles	Load Movement
1	Implanted	Normal	All	With; without	Defined by gait
2	Implanted native	Normal	16%	With	Defined by gait
3	Implanted	Normal	16%	With	Medial (+7 mm)–lateral (−1 mm); anterior–posterior (±14 mm)
4	Implanted	Normal trunk-sway	All	With	Defined by gait

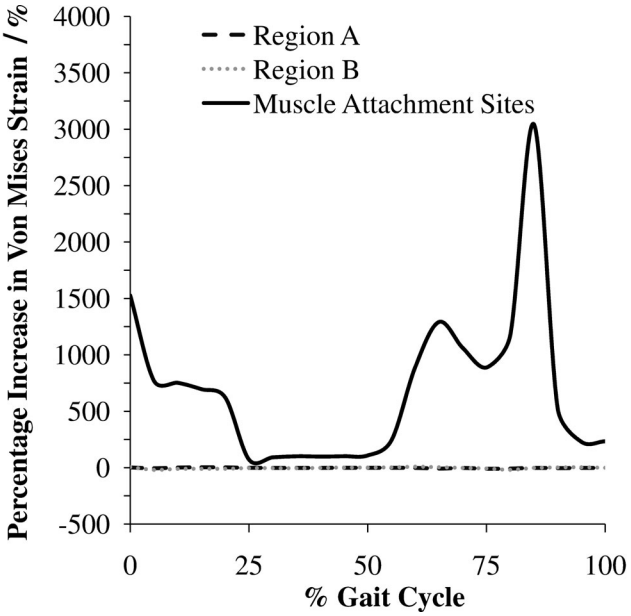

Figure 4. Average ΔVMS after the addition of muscle forces, results shown for Region A, Region B, and the muscle attachment sites. The analysis was performed with loading from a normal gait cycle, the mean values for the entire cycle are summarized.

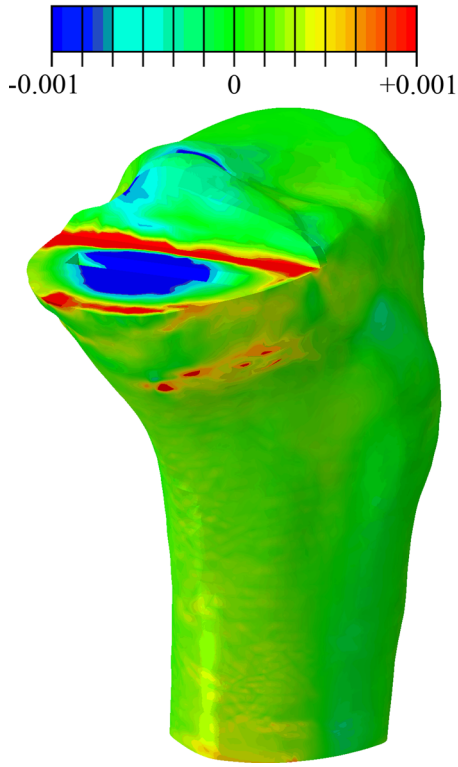

Figure 5. Regional ΔVMS strain after implantation.

Table 3. Mann–Whitney *U* Results Indicating the Significance (p) of the von Mises Strain Between the Model With, and Without, Muscle Forces, at Each Stage of the Gait Cycle

	p-Value	
% Gait Cycle	Region A	Region B
0	0.738	0.718
5	0.565	0.327
10	0.718	0.429
15	0.512	0.341
20	0.799	0.602
25	0.799	0.758
30	0.678	0.659
35	0.718	0.698
40	0.718	0.718
45	0.718	0.779
50	0.779	0.738
55	0.738	0.698
60	0.779	0.678
65	0.779	0.799
70	0.799	0.779
75	0.718	0.799
80	0.758	0.779
85	0.799	0.799
90	0.779	0.779
95	0.758	0.758
100	0.718	0.799

The analysis was performed on the two periprosthetic regions. No significant difference was found between the data ($p < 0.05$) at any stage.

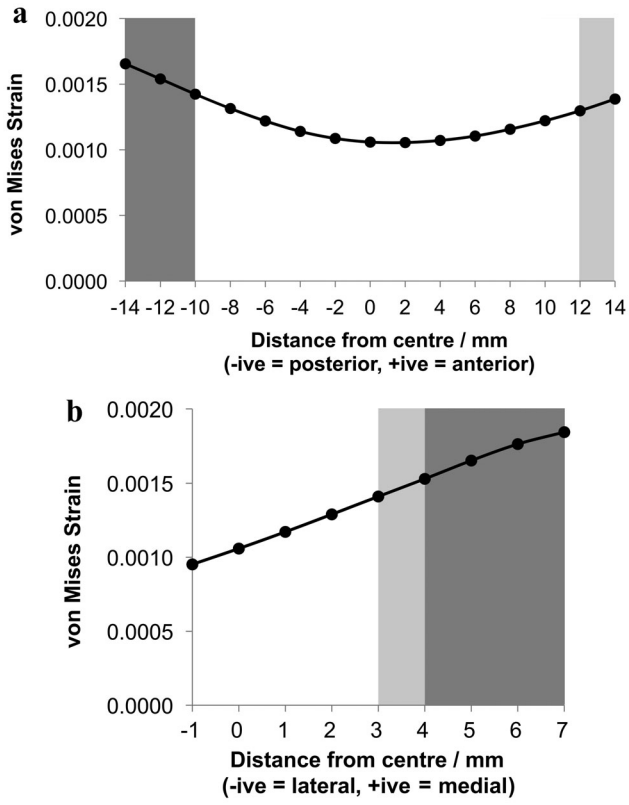

Figure 6. Illustration of the mean von Mises strain in Region A when the load position was moved from AP (a) and from ML (b). Significance between the von Mises strain at each distance compared with 0 mm distance are highlighted in light gray ($p < 0.05$) or dark gray ($p < 0.01$) as appropriate.

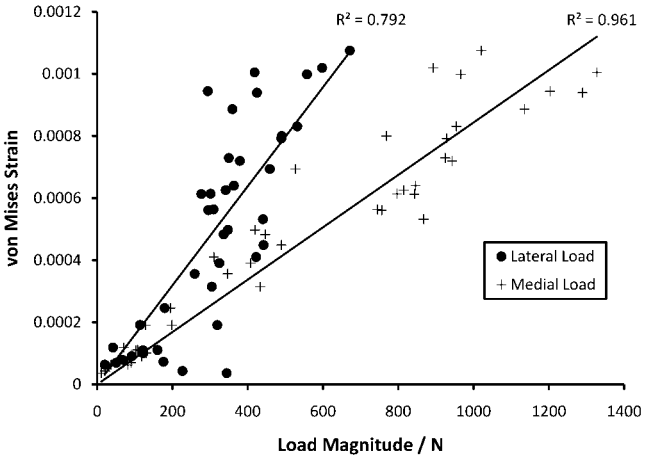

Figure 7. Curves illustrating the linear correlation between the medial and lateral load and the mean von Mises strain in Region A.

UKR. UKR implantation, loading position, and gait pattern all significantly affected tibial strains; however, muscle forces acting directly on the tibia did not affect strains within the periprosthetic region.

We failed to reject our hypothesis that adding muscle forces to a UKR simulation did not significantly affect tibial strain. However, our hypothesis was rejected for other regions in the model. For studies that only need to consider the periprosthetic region of a UKR, our findings indicate that the omission of muscle forces acting at their attachment sites on the tibia will not significantly affect the results.

Muscle forces play an important role in measured strains within the hip,[24–26] and the finding that muscle forces do not affect the periprosthetic region of the Oxford UKR highlights differences in muscular function between the two joints. The proximal femur is subjected to high bending forces due to the offset load, and the muscles surrounding the hip act to reduce these forces.[24] This function may not be as critical in the tibia. It should also be considered that muscle forces implicitly contribute to the joint contact forces,[27] and our study only removed the muscle forces from the attachment sites. Therefore, if the muscles act primarily to compress the joint, then no difference would be observed in tibial strains if muscular influence on contact force is not modeled. It is currently unknown whether this finding would hold true for a TKR or a lateral UKR.

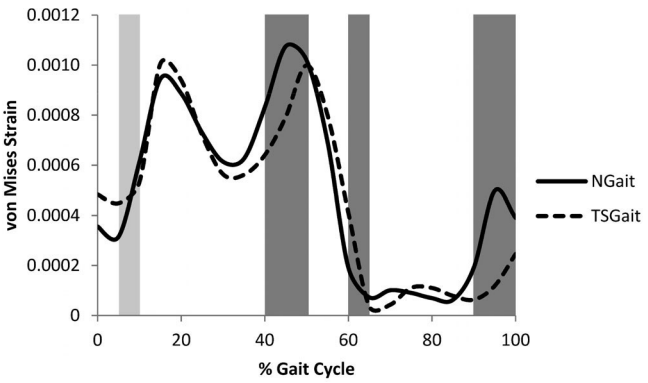

Figure 8. Variation in mean von Mises strain within Region A during normal gait (NGait) and lateral trunk-sway gait (TSGait). Significantly different results between the two gait trials, examined at each time interval, are highlighted in light gray ($p < 0.05$) or dark gray ($p < 0.01$) as appropriate.

The implantation of a UKR component increased the VMS within Region A by 20% during normal gait. A previous study found a larger increase in the same region (40%) during a stair climbing case that involved higher magnitude loads.[4] Whether this difference is due to the different load magnitude, the load condition, or the boundary conditions used is the subject of further study. A large increase in strain was also found in the corner between the sagittal and transverse bone cuts. This finding correlates with a study by Chang et al.,[28] and it is not surprising that the corner acts as a stress-raiser. A high density of bone is often observed on radiographs in this region after the bone has adapted (~1 year post-op).[29] The bone might remodel in response to a high strain energy density.[30] Another consideration is whether this high strain could be related to subsidence of the tibial component, a possible complication after UKR. The cause of subsidence is unknown, but some studies associate it with poor underlying bone quality,[31] incorrect component sizing,[32] or excessive underhang of the tibial component,[32] all of which would increase the strain within the corner. Unfortunately, the exact strain of a sharp corner cannot accurately be predicted using FE; a realistic curvature must be included. Therefore, no quantitative conclusions about subsidence can be drawn from our study; however, a future study is planned that will determine the curvature at the tibial corner and analyze a variety of tibias with varying bone quality to examine this possibility.

The bearing of the Oxford UKR is mobile and follows the position of the femoral component due to the fully congruent spherical articulating surfaces.[33] As a result, the position of the bearing on the tray varies during gait. But surgical factors also affect the load location. In addition to femoral component placement, tibial tray positioning is important because the tray wall limits lateral bearing movement. Correct tibial tray positioning affects clinical outcome.[4,32] For this reason, the positioning and orientation of the vertical cut should be correct, and the appropriate implant size should be used.

Positioning of the bearing, and therefore loading, in the AP direction was not found to affect periprosthetic tibial strain unless moved >10 mm posterior or 12 mm anterior from the center. A fluoroscopic study examining Oxford UKR bearing translation found bearing motion to be predominantly posterior to the center[34] with a maximum movement of 7 mm. Therefore, AP motion is not thought to significantly affect tibial strain.

However, in the ML direction, tibial strain increased the further medial the load was applied, and this effect became significant after only 3 mm of movement from the center, suggesting that surgical factors that may force the bearing medially to a distance of >3 mm, such as medial placement of the femoral component, should be avoided. The bearing position may also be moved medially by the use of a small tray in a large patient, or by medial placement of the vertical cut; however, these factors were not examined. Overhang of the tibial component beyond 3 mm increases the risk of poor patient outcome[32] and increases the strain within the tibia.[4] An overhanging component would be more likely to shift the load medially due to the resultant medial positioning of the tray wall, assuming constant component size. Thus, the increased strain observed in previous studies may be due to the shift in load position rather than the overhang itself.

Examination of the medial tibial VMS during normal gait and trunk-sway gait revealed a significant correlation with both medial and lateral load. The correlation was stronger for medial load, and multiple linear regressions revealed that medial load had a greater influence on tibial strain. Based on this finding, if tibial strain relates to post-op pain, then it may be possible to treat patients with pain non-invasively using gait modification techniques during the initial post-op period to reduce medial load or to transfer load more laterally. Other methods that reduce joint contact force, such as a reduction in patient activity or use of an off loader knee brace[35] may also help. Gait modification has been researched primarily as a tool to reduce arthritis progression by reducing the external knee adduction moment, an indirect measure of the medial load.[36] We found a slight (6%) reduction in tibial strain for a trunk-sway gait pattern compared with normal gait that was significant for the FE data. However, trial-to-trial variability in the gait data was not taken into account. Greater reductions might be achieved with different gait adaptations, such as using walking poles.[10]

The main limitation of this study is that the muscle forces were representative of only a specific situation. The forces were calculated based on motion data captured from a subject implanted with an instrumented TKR, and therefore represent an ACL deficient patient with an implanted knee. It was also assumed that the UKR loading conditions, which are largely unknown, are similar to those of a TKR. In this study, the load was applied directly to the bone rather than through cartilage, which may not represent the physiological situation. However, an indication for UKR is full thickness cartilage loss on the implanted side, and thus we assumed this representation to be reasonable for the one side; for the un-implanted side we assumed this side was sufficiently far from the regions of interest not to influence the result. Implantation of the component was simplified and did not account for pressurization and forces during insertion; these factors could have increased the strain further. Also, the cement thickness was assumed to be even around the implant.

Table 4. Details of the Subjects Used for the Musculoskeletal Model and the FE Simulations

Model	Gender	BMI	Age (y)
Musculoskeletal model	Male	22.5	83
FE simulation	Male	25.9	60

When assessing significance among models, an assumption was made that all of the variation within the models was caused by error in load magnitude; error in the load area and load position were not accounted for. We did not account for the effect of patient factors (e.g., gender, height, weight, age, or shape of the native tibia). The registration of the muscle forces onto a different tibia may have also introduced some error, but the two subjects were of similar stature (Table 4), and the error would be consistent throughout because all results were comparisons of simulations using the same tibia.

In summary, we assessed how a variety of factors affect tibial bone strain after UKR. Muscle forces applied to the attachment sites on the tibia were the only factor tested that did not cause a significant change. Strain was increased by implantation, by moving the implant loading medially, and by gait patterns resulting in higher medial loading. This indicates that clinically the incidence of pain after UKR might be reduced by improving surgical technique to ensure more lateral load positioning or by using gait modification techniques or a knee brace during rehabilitation to relieve symptoms.

ACKNOWLEDGMENTS

Some of the authors received funding from a commercial party, but this was unrelated to the present study. The authors thank Mrs. B. Marks (Nuffield Department of Orthopaedics, Rheumatology and Musculoskeletal Sciences, Oxford, UK) for her assistance.

REFERENCES

1. Pandit H, Jenkins C, Barker K, et al. 2006. The Oxford medial unicompartmental knee replacement using a minimally-invasive approach. J Bone Joint Surg Br 88:54–60.
2. O'Brien S, Bennett D, Doran E, et al. 2009. Comparison of hip and knee arthroplasty outcomes at early and intermediate follow-up. Orthopedics 32:168–168.
3. Brianza S, Brighenti V, Lansdowne JL, et al. 2011. Finite element analysis of a novel pin-sleeve system for external fixation of distal limb fractures in horses. Vet J 190:260–267.
4. Simpson DJ, Price AJ, Gulati A, et al. 2009. Elevated proximal tibial strains following unicompartmental knee replacement—a possible cause of pain. Med Eng Phys 31:752–757.
5. Kaufman KR, An KN, Litchy WJ, et al. 1991. Physiological prediction of muscle forces—I. Theoretical formulation. Neuroscience 40:781–792.
6. Lloyd DG, Besier TF. 2003. An EMG-driven musculoskeletal model to estimate muscle forces and knee joint moments in vivo. J Biomech 36:765–776.

7. Buchanan TS, Lloyd DG, Manal K, et al. 2005. Estimation of muscle forces and joint moments using a forward-inverse dynamics model. Med Sci Sports Exerc 37:1911–1916.
8. Lin Y-C, Walter JP, Banks SA, et al. 2010. Simultaneous prediction of muscle and contact forces in the knee during gait. J Biomech 43:945–952.
9. D'Lima DD, Townsend CP, Arms SW, et al. 2005. An implantable telemetry device to measure intra-articular tibial forces. J Biomech 38:299–304.
10. Fregly BJ, D'Lima DD, Colwell CW. 2009. Effective gait patterns for offloading the medial compartment of the knee. J Orthop Res 27:1016–1021.
11. Fregly BJ, Besier TF, Lloyd DG, et al. 2012. Grand challenge competition to predict in vivo knee loads. J Orthop Res 30:503–513.
12. Mündermann A, Asay JL, Mündermann L, et al. 2008. Implications of increased medio-lateral trunk sway for ambulatory mechanics. J Biomech 41:165–170.
13. Bei Y, Fregly BJ. 2004. Multibody dynamic simulation of knee contact mechanics. Med Eng Phys 26:777–789.
14. Delp SL, Anderson FC, Arnold AS, et al. 2007. OpenSim: open-source software to create and analyze dynamic simulations of movement. IEEE Trans Biomed Eng 54: 1940.
15. Arnold E, Ward S, Lieber R, et al. 2010. A model of the lower limb for analysis of human movement. Ann Biomed Eng 38:269–279.
16. Walter JP, D'Lima DD, Besier TF, et al. 2011. Feasibility of highly constrained muscle force predictions for the knee during gait. In ASME Summer Bioengineering Conference. Pennsylvania, USA.
17. Gray HA, Taddei F, Zavatsky AB, et al. 2008. Experimental validation of a finite element model of a human cadaveric tibia. J Biomech Eng 130:031016.
18. Besl PJ, McKay HD. 1992. A method for registration of 3-D shapes. IEEE Trans Pattern Anal 14:239–256.
19. Biomet. 2007. Oxford partial knee manual of the surgical technique. Bridgend: Biomet UK Ltd.
20. Walker PS, Hajek JV. 1972. The load-bearing area in the knee joint. J Biomech 5:581–589.
21. Feng G, Qu S, Huang Y, et al. 2007. An analytical expression for the stress field around an elastoplastic indentation/contact. Acta Materialia 55:2929–2938.
22. Dar FH, Meakin JR, Aspden RM. 2002. Statistical methods in finite element analysis. J Biomech 35:1155–1161.
23. Janssen D, Mann KA, Verdonschot N. 2009. Finite element simulation of cement-bone interface micromechanics: a comparison to experimental results. J Orthop Res 27:1312–1318.
24. Duda GN, Heller M, Albinger J, et al. 1998. Influence of muscle forces on femoral strain distribution. J Biomech 31: 841–846.
25. Polgar K, Gill HS, Viceconti M, et al. 2003. Strain distribution within the human femur due to physiological and simplified loading: finite element analysis using the muscle standardized femur model. Proc Inst Mech Eng [H] 217:173.
26. Stolk J, Verdonschot N, Huiskes R. 2001. Hip-joint and abductor-muscle forces adequately represent in vivo loading of a cemented total hip reconstruction. J Biomech 34:917–926.
27. Herzog W, Longino D, Clark A. 2003. The role of muscles in joint adaptation and degeneration. Langenbeck Arch Surg 388:305–315.
28. Chang T-W, Yang C-T, Liu Y-L, et al. 2011. Biomechanical evaluation of proximal tibial behavior following unicondylar knee arthroplasty: modified resected surface with corresponding surgical technique. Med Eng Phys 33:1175–1182.
29. Pandit H, Jenkins C, Beard DJ, et al. 2009. Cementless Oxford unicompartmental knee replacement shows reduced radiolucency at one year. J Bone Joint Surg Br 91-B:185–189.
30. Huiskes R, Weinans H, Grootenboer HJ, et al. 1987. Adaptive bone-remodeling theory applied to prosthetic-design analysis. J Biomech 20:1135–1150.
31. Vardi G, Strover AE. 2004. Early complications of unicompartmental knee replacement: the Droitwich experience. Knee 11:389–394.
32. Chau R, Gulati A, Pandit H, et al. 2009. Tibial component overhang following unicompartmental knee replacement—Does it matter? Knee 16:310–313.
33. Goodfellow JW, O'Connor JJ, Dodd CAF, et al. 2006. Unicompartmental arthroplasty with the Oxford knee. Oxford: Oxford University Press.
34. Pandit H, Van Duren BH, Gallagher JA, et al. 2008. Combined anterior cruciate reconstruction and Oxford unicompartmental knee arthroplasty: in vivo kinematics. Knee 15:101–106.
35. Pollo FE, Otis JC, Backus SI, et al. 2002. Reduction of medial compartment loads with valgus bracing of the osteoarthritic knee. Am J Sports Med 30:414–421.
36. Simic M, Hinman RS, Wrigley TV, et al. 2011. Gait modification strategies for altering medial knee joint load: a systematic review. Arthritis Care Res 63:405–426.